Letter

UV photoconductivity characteristics of ZnO nanowire field effect transistor treated by proton irradiation

Minhyeok Choe [a], Woong-Ki Hong [b,1], Woojin Park [a], Jongwon Yoon [a], Gunho Jo [a,2], Taehyeon Kwon [b], Mark E. Welland [c], Takhee Lee [d,*]

[a] School of Materials Science and Engineering, Gwangju Institute of Science and Technology, Gwangju 500-712, Republic of Korea
[b] Department of Nanobio Materials and Electronics, Gwangju Institute of Science and Technology, Gwangju 500-712, Republic of Korea
[c] Nanoscience Centre, University of Cambridge, Cambridge CB3 0FF, UK
[d] Department of Physics and Astronomy, Seoul National University, Seoul 151-747, Republic of Korea

ABSTRACT

We investigated the UV photoconductivity characteristics of ZnO nanowire field effect transistors (FETs) ir-radiated by proton beams. After proton beam irradiation (using a beam energy of 10 MeV and a fluence of 10^{12} cm^{-2}), the drain current and carrier density in the ZnO nanowire FETs decreased, and the threshold voltage shifted to the positive gate bias direction due to the creation of interface traps at the SiO$_2$/ZnO nano-wire interface by the proton beam. The interface traps produced a higher surface barrier potential and a larg-er depletion region at the ZnO nanowire surface, affecting the photoconductivity and its decay time. The UV photoconductivity of the proton-irradiated ZnO nanowire FETs was higher and more prolonged than that of the pristine ZnO nanowire FETs. The results extend our understanding of the UV photoconductivity charac-teristics of ZnO nanowire devices and other materials when irradiated with highly energetic particles.

© 2012 Elsevier B.V. All rights reserved.

1. Introduction

ZnO nanowires have been versatile materials with interesting elec-trical, chemical, and optical properties including piezoelectric transport characteristics, gas and ultraviolet (UV) sensing capabilities, and trans-parency with light absorption [1–5]. In particular, ZnO nanowires, which have a wide direct bandgap (~3.4 eV) and a large exciton binding energy (~60 meV), have excellent UV photoconductivity characteristics under widely varying environments, such as vacuum, nitrogen, oxygen, and water [6–8]. The UV photoconductivity of ZnO nanowires is influ-enced by the adsorption and desorption of gas molecules on the surface. For example, under UV illumination, electron–hole pairs are created in the nanowire ($h\nu \to e^- + h^+$). The photogenerated holes recombine with adsorbed oxygen ions and allow them to detach from the nano-wire surface, creating an excess of electrons in the nanowire ($e^- + h^+ + O_2^-(ad) \to e^- + O_2(g)$). These excess electrons contribute to an increase in photoconductivity. However, when UV light is turned off, these electrons recombine with oxygen molecules on the surface of nanowire ($e^- + O_2(g) \to O_2^-(ad)$), leading to photocurrent decay. These conductivity phenomena for nanowire surfaces interacting with gas molecules have been reported in many studies [9–14].

Nevertheless, it remains important to attain a more thorough study of the UV photoconductivity characteristics of nanowires, especially for the UV photoresponse effect of the interface states on ZnO nanowires. To this end, we introduced the irradiation-mediated engineering, which can be used for the property-tailoring of nanomaterials and de-vices [15–19]. For example, our previous work demonstrated the tun-ing of the electrical characteristics of ZnO nanowire field effect transistors (FETs) by proton irradiation [20,21].

In this study, we investigated the UV photoconductivity character-istics of ZnO nanowire FETs treated by proton irradiation. After irradi-ation with a high-energy proton beam, the threshold voltage of the ZnO nanowire FETs shifted in the positive gate bias direction due to the formation of proton-induced interface traps at the SiO$_2$/ZnO nanowire interface. In particular, we studied the UV photoconductiv-ity characteristics of the proton-irradiated ZnO nanowire FETs in comparison with that of the pristine ZnO nanowire FETs.

2. Experimental details

The synthesis of the ZnO nanowires was as follows: Au-coated c-plane sapphire substrates with commercially available ZnO powder (99.995%) and graphite powder (99%) with a ratio of 1:1 were placed into a chemical vapor deposition chamber that was maintained at 93.3 kPa and heated to 900 °C under a flow of mixed argon and oxygen gases. After the growth of the ZnO nanowires, sonication in isopropyl al-cohol solution was performed to detach them from the growth sub-strate, and the resulting nanowire suspension was then deposited

---

onto a silicon wafer to fabricate ZnO nanowire FETs. A 300-nm-thick, thermally grown SiO_2 layer was used as a gate insulator on a heavily doped p-type silicon substrate. Metal electrodes consisting of Ti/Au (30/50 nm) were deposited on the ZnO nanowires with an electron beam evaporator and patterned as source and drain electrodes via a photolithography process. A more detailed description of the ZnO nanowire synthesis and FET device fabrication has been published elsewhere [20]. Fig. 1(a) shows a field emission scanning electron microscopy (FESEM) image of a ZnO nanowire connected between the source and drain electrodes in a typical back-gate FET device structure (Fig. 1(b)). The inset of Fig. 1(a) shows ZnO nanowires vertically grown on a sapphire substrate. The accelerating voltage and emission current of FESEM are 10 kV and 20 μA, respectively.

For proton irradiation of the ZnO nanowire FETs, accelerated proton beams were generated using an MC-50 cyclotron (at the Korean Institute of Radiological and Medical Sciences, Korea), with a proton beam energy of 10 MeV and a fluence of 10^{12} cm^{-2}. The average beam current was 10 nA, and the irradiated area was 5×5 cm^2 with a uniformity of ~90% or better. The high energetic proton beam irradiation can produce the electron–hole pairs in SiO_2, but does not impact ZnO layer directly [20–25]. The radiation-induced holes in SiO_2 layer enhances gate electric field, or some of the radiation-induced holes transport to the SiO_2/ZnO interface acting as trap sites at the interface, which will eventually influence the electric properties of ZnO nanowire FETs.

The electrical properties of the ZnO nanowire FETs were systematically characterized before and after the proton irradiation using a semiconductor parameter analyzer (Agilent B1500A) at room temperature. The UV photoconductivity properties of the ZnO nanowire FETs were examined using a portable UV lamp with a 365-nm emission at a power of 0.7 mW/cm^2 as the excitation source.

3. Results and discussion

3.1. Electrical characteristics of ZnO nanowire FETs

The representative transfer characteristics (drain current versus gate voltage, I_{DS}–V_G) and output characteristics (drain current versus drain voltage, I_{DS}–V_{DS}) of the ZnO nanowire FETs before proton irradiation are shown in Fig. 1(c) and (d). The transfer curves in Fig. 1(c) were measured at drain voltages varying from 0.1 to 1 V in increments of 0.3 V. The results display conventional enhancement-mode n-type ZnO nanowire FET characteristics, i.e., a zero off-current at zero gate voltage and a positive threshold voltage [26]. The threshold voltage at a fixed drain voltage of 1.0 V was ~5.0 V, as determined by extrapolating the linear portion of the maximum slope to the zero drain current; here, the point of maximum slope is the point at which the transconductance ($g_m = dI_{DS}/dV_G$) is maximal [20]. The output curves in Fig. 1(d) were measured at gate voltages varying from −9 to 15 V in increments of 6 V. The drain current of the ZnO nanowire FETs increased proportionally to the applied drain voltage within the linear regime at low bias and changed little with the applied drain voltage in the saturation regime at high bias. These results indicate that our ZnO nanowires performed as standard n-channel FETs.

The ZnO nanowire FETs were then exposed to proton beam irradiation. To perform a systematic and accurate comparison before and after proton irradiation, we sequentially measured the electrical characteristics of a ZnO nanowire FET before proton irradiation (denoted as "pristine", Fig. 2(a) top) and after proton irradiation (denoted as "proton", Fig. 2(a) middle), and then under UV illumination (denoted as "proton & UV", Fig. 2(a) bottom). Three different experimental conditions were carried out on the same ZnO nanowire FET. The drain current decreased after proton irradiation; for example, the current measured at $V_{DS} = 10$ V and $V_G = 15$ V decreased from 5.05 μA before proton irradiation to 4.38 μA after irradiation. The reduction of drain current was observed similarly in our previous reports, which is attributed to high energy proton irradiation effect [20,21].

The current reduction was accompanied by a threshold voltage shift; in our case, the threshold voltage shifted from 5.4 to 8.0 V after proton irradiation (Fig. 2(b)). This indicates that a more positive gate voltage was required for the proton-irradiated ZnO nanowire FETs than for the pristine ZnO nanowire FETs. The threshold voltage can be used to estimate the carrier concentration from the total charge, $Q_{tot} = C_G |V_G - V_{th}|$, in the nanowire, where C_G is the gate capacitance and V_{th} is the threshold voltage [27]. The gate capacitance

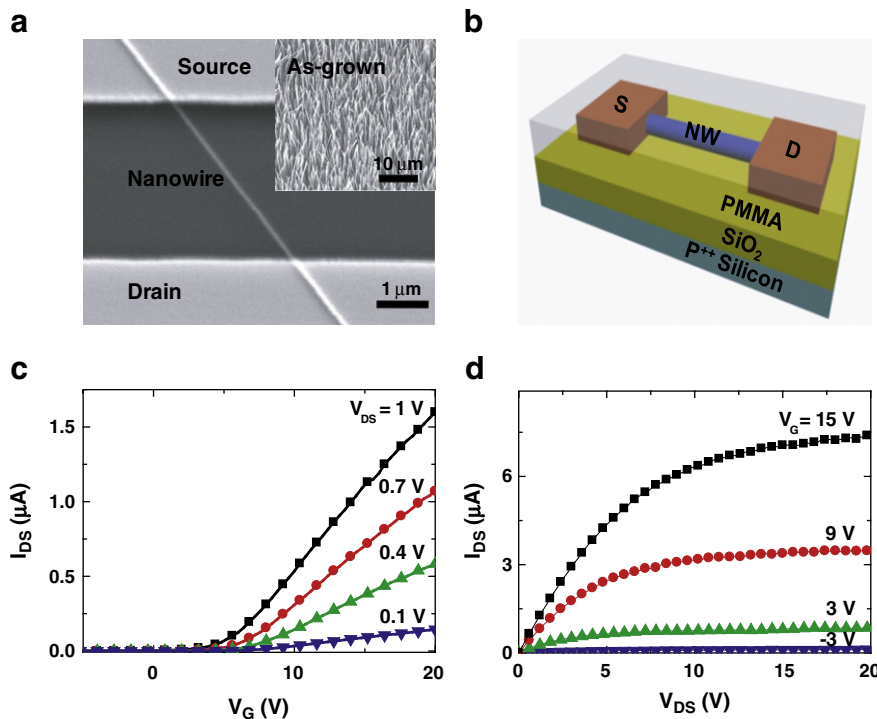**a**　　　　**b**

c　　　　**d**

Fig. 1. (a) FESEM images of a ZnO nanowire FET and vertically grown ZnO nanowires (inset). (b) Schematic of a ZnO nanowire FET. (c) Transfer characteristics (I_{DS}–V_G) for drain voltages varying from 0.1 to 1 V in increments of 0.3 V. (b) Output characteristics (I_{DS}–V_{DS}) for gate voltages varying from −9 to 15 V in increments of 6 V.
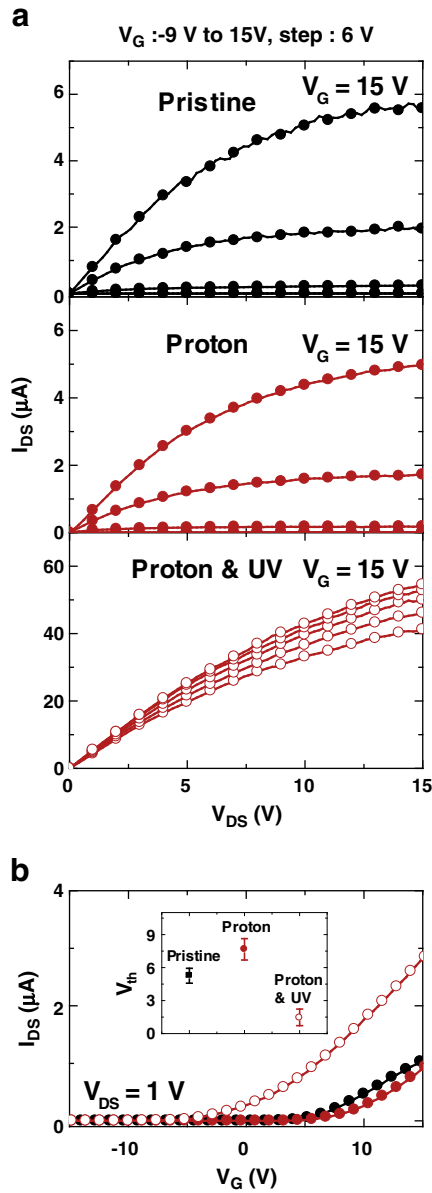
Fig. 2. (a) A series of I_{DS}–V_{DS} curves for ZnO nanowire FETs before proton irradiation (top), after proton irradiation (middle), and when illuminated with UV light after proton irradiation (bottom) for gate voltages varying from −9 to 15 V with an increment of 6 V. (b) I_{DS}–V_G curves for ZnO nanowire FETs at a fixed $V_{DS} = 1$ V. The inset shows the statistical distribution of the threshold voltages for the three cases (see text).

Therefore, the main effect observed after proton irradiation was that the current and carrier concentration of the ZnO nanowire FETs were reduced and that the threshold voltage shifted in the positive gate bias direction. However, we note that the proton irradiation effect on these devices would be different from the suspended-type ZnO nanowire FET where the ZnO nanowires are suspended over the substrate [20]. Unlike the devices where the ZnO nanowires are placed on the substrate, in the case of suspended-type ZnO nanowire FETs there is no effect by the interface traps at the SiO_2/ZnO nanowire interface due to the absence of irradiation-induced interface states [20].

In addition, to study the UV photoconductivity effects, the proton-irradiated ZnO nanowire FETs were illuminated with UV light at a wavelength of 365 nm, thus creating electron–hole pairs in the ZnO nanowires. When the proton-irradiated ZnO nanowire FETs were exposed to UV light, the drain current (Fig. 2(a) bottom) dramatically increased, and the threshold voltage significantly shifted to the negative gate bias direction; for example, the threshold voltage shifted from 8.0 to 1.1 V upon UV illumination (Fig. 2(b)). The threshold voltage shift in the negative gate bias direction indicates that a lower gate voltage was able to produce conducting channels in the ZnO nanowires. The excess photogenerated electron–hole pairs contributed to an enhanced carrier concentration ($\sim 9.08 \times 10^{17}$ cm^{-3} at the same gate voltage of 15 V after UV illumination). The inset of Fig. 2(b) shows the statistical values of the threshold voltage for the ZnO nanowire FETs in three cases: pristine (5.3 ± 0.7 V), proton (7.7 ± 1.0 V), and proton & UV (1.4 ± 0.8 V). The error bars in this plot were obtained from measurements of five different ZnO nanowire FETs in each case. In summary, we observed that the threshold voltage shifted to the positive gate bias direction due to proton irradiation and then shifted to the negative gate bias direction due to UV illumination.

3.2. Analysis of UV photoconductivity and decay time

The photoconductivity of ZnO nanowires has been explained mainly by two processes; one process involves photogenerated electron–hole pairs, and another is related to surface states on the ZnO nanowire surface. We measured the UV photocurrent responses of the pristine and proton-irradiated ZnO nanowire FET at a fixed $V_G = 0$ V and a fixed $V_{DS} = 1$ V, as shown in Fig. 3. Also, the UV photocurrent responses of the pristine and proton-irradiated ZnO nanowire FET were carried out on the same ZnO nanowire FET. We observed that the UV photoconductivity of the proton-irradiated ZnO nanowire FETs was higher than that of the pristine ZnO nanowire FETs (i.e., before proton irradiation). This was attributed to the formation of interface traps at the SiO_2/ZnO nanowire interface by the proton beam. As

C_G can be estimated using the model of a cylinder on an infinite metal plate, for which $C_G = 2\pi\varepsilon_0\varepsilon_r L / \cosh^{-1}(1 + h/r)$; here, r is the nanowire radius ($\sim$50 nm), L is the nanowire channel length ($\sim$4 μm), h is the SiO_2 thickness ($\sim$300 nm), ε_0 is the permittivity of free space, and ε_{SiO2} is the dielectric constant of SiO_2 ($\sim$3.9). The carrier concentration can roughly be estimated from Eq. (1) although the electrons may not be uniformly distributed throughout the entire ZnO nanowire channel.

$$n_e = \frac{Q_{tot}}{e\pi r^2 L} \tag{1}$$

The carrier concentrations at the arbitrarily chosen gate voltage of 15 V were calculated as 6.29×10^{17} cm^{-3} and 4.59×10^{17} cm^{-3} for the ZnO nanowire FET before and after proton irradiation, respectively.
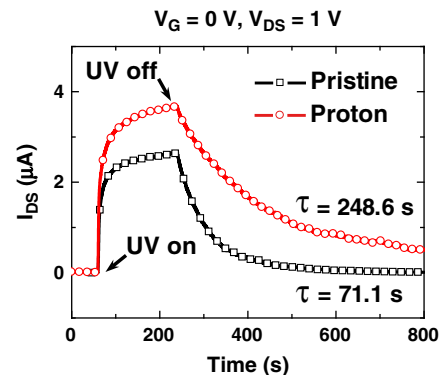

Fig. 3. Photoconductivity responses of pristine and proton-irradiated ZnO nanowire FETs under UV illumination at fixed gate voltage of 0 V and fixed drain voltage of 1 V.

we previously reported, high-energy proton irradiation produces interface traps in a dielectric layer [20,21], and these interface traps collect positive charge carriers in ZnO nanowires. For the proton-irradiated ZnO nanowire FETs under UV light, the photogenerated holes are captured by interface traps, and the photogenerated electrons are freely transferred in the ZnO nanowire, resulting in increased photoconductivity. A more detailed explanation will be provided later, utilizing the schematic illustration of energy band diagrams in Fig. 4.

In addition, after UV light off, the decay time of photocurrent is extracted from "pristine" and "proton" ZnO nanowire FET and is expressed as a simple exponential decay function of the form [28–30]:

$$I = I_0 \exp\left(\frac{-t}{\tau}\right) \qquad (2)$$

Here, the decay time τ for the ZnO nanowire FET was estimated at 71.1 s and 248.6 s before and after proton irradiation, respectively. The decay time is related to the recombination of electron–hole pairs, which is influenced by interface traps because they can capture the photogenerated holes in the ZnO nanowires produced under UV light. However, when the UV light is turned off, the photogenerated electrons and holes recombine. The presence of holes trapped in interface traps hinders the recombination of electron–hole pairs. Therefore, the decay of photoconductivity is prolonged by the slower recombination of photogenerated electron–hole pairs. In a related study, it was reported that the photocurrent decay rate of ZnO nanowire FETs is higher in air than in vacuum [12]; this effect is due to the relatively higher adsorption rates of oxygen molecules and water vapor in the air than in a vacuum. Both adsorbed oxygen molecules and water vapor can capture and combine with electrons transferred from nanowire.
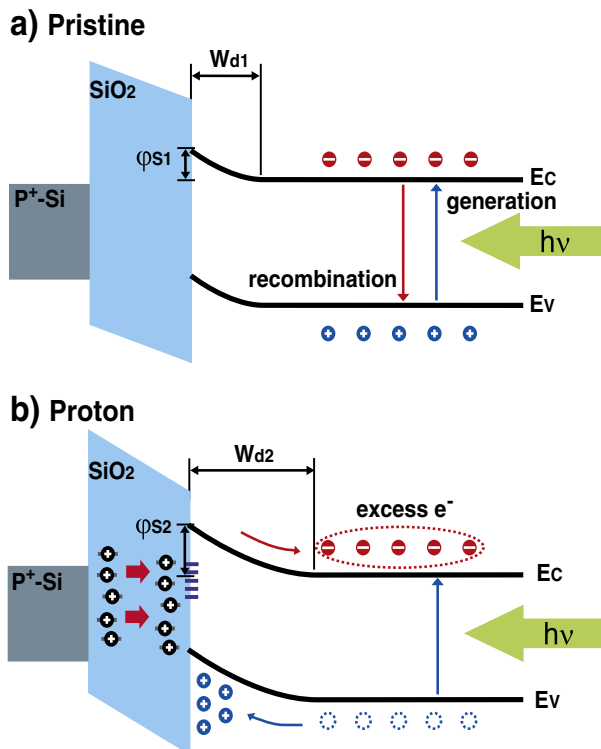
A higher adsorption rate of gas molecules indicates a higher recombination rate of electron–hole pairs. Consequently, the decay of photoconductivity characteristics is attributed to the recombination rate of trapped electron–hole pairs at the interface.

3.3. Photoconductivity mechanism in proton-irradiated ZnO nanowires

Fig. 4 shows schematic energy band diagrams of the pristine and proton-irradiated ZnO nanowire FETs under UV illumination. We have previously explained the energy band diagrams for ZnO nanowire FET to verify the proton irradiation effect [20]. For the pristine ZnO nanowire FET represented in Fig. 4(a), the electronic conduction (E_C) and valence (E_V) bands illustrate surface-band bending, with a surface depletion width (W_{d1}) and a surface barrier potential (φ_{s1}), at the SiO_2/ZnO nanowire interface. In contrast, for the proton-irradiated ZnO nanowire FET corresponding to Fig. 4(b), the electronic band displays surface-band bending with a relatively larger surface depletion width (W_{d2}) and a higher surface barrier potential (φ_{S2}) than those of pristine ZnO nanowire FET due to the irradiation-induced interface traps [20]. As the surface depletion width is enlarged by interface traps, as shown in Fig. 4(b), a higher gate electric field is needed to create the conducting channel in the ZnO nanowire, and thus, the threshold voltage shifts toward the positive gate bias direction [20]. When the proton-irradiated ZnO nanowire FET was exposed to UV light, the threshold voltage shifted toward the negative gate bias direction due to the presence of excess electrons, as shown in Fig. 4(b). This shift is consistent with our observations of a threshold voltage shift and a current change (Fig. 2). In addition, the photoconductivity and its decay time in the proton-irradiated ZnO nanowire FETs can be explained by the surface-band bending. When the UV light is off, the recombination of photogenerated electron–hole pairs in the proton-irradiated ZnO nanowire FETs is disturbed by the relatively larger depletion width and higher surface potential barrier as compared to those in the pristine ZnO nanowire FETs. Therefore, the recombination of electron–hole pairs in the proton-irradiated ZnO nanowire FET is slower than in the pristine ZnO nanowire FET. Consequently, these results indicate that the interface traps produced by high-energy proton irradiation are expected to play an important role in the enhancement of photoconductivity and the increase in photocurrent decay time.

4. Conclusions

We investigated the UV photoconductivity of ZnO nanowire FETs treated by proton beam irradiation. The proton-irradiated ZnO nanowire FETs exhibited interface traps at the SiO_2/ZnO nanowire interface, which resulted in a decrease in the drain current and a threshold voltage shift toward the positive gate bias direction. When electron–hole pairs were created under UV light, the photogenerated holes were trapped in the interface traps, increasing the photocurrent due to the excess photogenerated electrons. And when UV light was turned off, the recombination of photogenerated electron–hole pairs is delayed by the relatively larger depletion width and higher surface potential barrier in the proton-irradiated ZnO nanowire FETs, resulting in an extended decay time of photocurrent. This study extends our understanding of the correlation of interface traps and photoconductivity characteristics in ZnO nanowire devices and other materials.

Fig. 4. Energy band diagrams of (a) pristine and (b) proton-irradiated ZnO nanowire FETs under UV illumination.

References

[1] J. Goldberger, D.J. Sirbuly, M. Law, P. Yang, J. Phys. Chem. B 109 (2005) 9.
[2] X. Wang, J. Zhou, J. Song, J. Liu, N. Xu, Z.L. Wang, Nano Lett. 6 (2006) 2768.
[3] H. Tong, B.-L. Wang, Z.-C. Ou-Yang, Thin Solid Films 516 (2008) 2708.
[4] C. Soci, A. Zhang, B. Xiang, S.A. Dayeh, D.P.R. Aplin, J. Park, X.Y. Bao, Y.H. Lo, D. Wang, Nano Lett. 7 (2007) 1003.
[5] L. Hu, G. Chen, Nano Lett. 7 (2007) 3249.
[6] H. Kind, H. Yan, B. Messer, M. Law, P. Yang, Adv. Mater. 14 (2002) 158.
[7] X.J. Zheng, B. Yang, T. Zhang, C.B. Jiang, S.X. Mao, Y.Q. Chen, B. Yuan, Appl. Phys. Lett. 95 (2009) 221106.
[8] S. Song, W.-K. Hong, S.-S. Kwon, T. Lee, Appl. Phys. Lett. 92 (2008) 263109.
[9] V. Khranovskyy, J. Eriksson, A. Lloyd-Spetz, R. Yakimova, L. Hultman, Thin Solid Films 517 (2009) 2073.
[10] Q.H. Li, T. Gao, Y.G. Wang, T.H. Wang, Appl. Phys. Lett. 86 (2005) 123117.
[11] R.S. Chen, C.Y. Lu, K.H. Chen, L.C. Chen, Appl. Phys. Lett. 95 (2009) 233119.
[12] J.B.K. Law, J.T.L. Thong, Appl. Phys. Lett. 88 (2006) 133114.
[13] H.M. Huang, R.S. Chen, H.Y. Chen, T.W. Liu, C.C. Kuo, C.P. Chen, H.C. Hsu, L.C. Chen, K.H. Chen, Y.J. Yang, Appl. Phys. Lett. 96 (2010) 062104.
[14] C.-H. Lin, R.-S. Chen, T.-T. Chen, H.-Y. Chen, Y.-F. Chen, K.-H. Chen, L.-C. Chen, Appl. Phys. Lett. 93 (2008) 112115.
[15] H.J. Barnaby, IEEE Trans. Nucl. Sci. 53 (2006) 3103.
[16] A.V. Krasheninnikov, F. Banhart, Nat. Mater. 6 (2007) 723.
[17] F. Banhart, Rep. Prog. Phys. 62 (1999) 1181.
[18] D. Teweldebrhan, A.A. Balandin, Appl. Phys. Lett. 94 (2009) 013101.
[19] A. Vijayaraghavan, K. Kanzaki, S. Suzuki, Y. Kobayashi, H. Inokawa, Y. Ono, S. Kar, P.M. Ajayan, Nano Lett. 5 (2005) 1575.
[20] W.-K. Hong, G. Jo, J.I. Sohn, W. Park, M. Choe, G. Wang, Y.H. Kahng, M.E. Welland, T. Lee, ACS Nano 4 (2010) 811.
[21] G. Jo, W.-K. Hong, J.I. Sohn, M. Jo, J. Shin, M.E. Welland, H. Hwang, K.E. Geckeler, T. Lee, Adv. Mater. 21 (2009) 2156.
[22] G. Yaron, A. Many, Y. Goldstein, J. Appl. Phys. 58 (1985) 3508.
[23] G. Yaron, J. Levy, Y. Goldstein, A. Many, J. Appl. Phys. 59 (1986) 1232.
[24] C. Coskun, D.C. Look, G.C. Farlow, J.R. Sizelove, Semicond. Sci. Technol. 19 (2004) 752.
[25] T.R. Oldham, F.B. Mclean, IEEE Trans. Nucl. Sci. 50 (2003) 483.
[26] A.S. Seda, K.C. Smith, Microelectronic Circuits, 5th edition Oxford University Press, 2003.
[27] M. Choe, G. Jo, J. Maeng, W.-K. Hong, M. Jo, G. Wang, W. Park, B.H. Lee, H. Hwang, T. Lee, J. Appl. Phys. 107 (2010) 034504.
[28] J.D. Prades, R. Jimenez-Diaz, F. Hernandez-Ramirez, L. Fernandez-Romero, T. Andreu, A. Cirera, A. Romano-Rodriguez, A. Cornet, J.R. Morante, S. Barth, S. Mathur, J. Phys. Chem. C 112 (2008) 14639.
[29] P. Gao, Z.Z. Wang, K.H. Liu, Z. Xu, W.L. Wang, X.D. Bai, E.G. Wang, J. Mater. Chem. 19 (2009) 1002.
[30] R. Ghosh, D. Basak, Appl. Phys. Lett. 90 (2007) 243106.